Evaluation of the Mechanical Properties of AA 6063 Processed by Severe Plastic Deformation

DAVOUD MASHHADI JAFARLOU, ERFAN ZALNEZHAD, ABDELMAGID SALEM HAMOUDA, GHADER FARAJI, NOOR AZIZI BIN MARDI, and MOHSEN ABDELNAEIM HASSAN MOHAMED

In this study, the mechanical properties, including surface hardness, tensile strength, fatigue, and fretting fatigue behavior of AA 6063 processed by equal channel angular pressing as the most efficient severe shear plastic deformation (SPD) technique, were investigated. Following the SPD process, samples were subjected to heat treatment (HT), hard anodizing (HA), and a combination of HT and HA. Rotating–bending fretting fatigue tests were performed to explore the samples' response to the fretting condition. From the experimental fatigue and fretting fatigue tests, it was apparent that the SPD treatment had a positive effect on enhancing the fatigue and fretting fatigue lives of the samples at low and high-cyclic loads compared with the HT technique by 78 and 67 pct, and 131 and 154 pct respectively. The results also indicate that the SPD + HT technique significantly increased the fatigue and fretting fatigue lives of the samples at high and low cycles by 15.56 and 8.33 pct, and 14.4 and 5.1 pct respectively, compared with the SPD method. HA of AA6063 increased the fatigue and fretting fatigue lives of SPD + HT-processed samples at low cycle by 15.5 and 18.4 pct respectively; however, at high cycle, HA had reverse effects, whereby the fatigue and fretting fatigue lives of SPD + HT-processed samples decreased by 16.7 and 30 pct, respectively.

DOI: 10.1007/s11661-015-2806-7
© The Minerals, Metals & Materials Society and ASM International 2015

I. INTRODUCTION

ALUMINUM alloy 6063 (AA 6063) is widely used in different industrial fields such as construction and transportation due to its acceptable formability, proper weldability, and corrosion resistance. However, the mechanical properties of this alloy such as hardness, tensile strength, fatigue life, and fretting fatigue behavior are not appreciable.[1]

Fretting is a contact damage process that occurs when fatigue load is imposed on a component, while it is in contact with an adjacent component. This phenomenon leads to oscillatory microslipping at the components' surfaces, which actuates the existing crack nucleation and eventually leads to unanticipated structure failure.[2,3]

A traditional fretting fatigue improvement strategy is coating as a surface modification method in industrial applications wherever contact parts are subjected to small amplitude relative motion as a result of vibration or cyclic loads. The effects of hard and soft coatings on fretting fatigue behavior have been studied broadly.[4]

In order to reduce the detrimental effect of fretting fatigue, hard anodizing (HA) is extensively applied in industry as an efficient coating technique. In addition, HA coating significantly increases surface hardness and corrosion resistance, and further simultaneously serves decorative purposes.[5]

The other technique for improving the mechanical properties of metallic materials is to decrease the metal grain size by subjecting them to severe shear plastic deformation (SPD). Bulk materials with ultrafine grains (UFGs) processed with SPD have attracted great interest in the industrial field for their unique mechanical properties. The major role of the SPD process is the imposition of ultra-large shear plastic strain into the material structure to convert coarse-grained (CG) structure into UFG structure.[6]

Various types of SPD techniques such as equal channel angular pressing (ECAP),[7] high-pressure torsion (HPT),[8] accumulative roll bonding (ARB),[9] cyclic extrusion compression (CEC),[10] repetitive tube expansion and shrinking (RTES),[11] and repetitive corrugation and straightening (RCS)[12] have been developed for UFG metal fabrication.

DAVOUD MASHHADI JAFARLOU, Researcher, ERFAN ZALNEZHAD and NOOR AZIZI BIN MARDI, Senior Lecturers, are with the Department of Mechanical Engineering, Faculty of Engineering, University of Malaya, 50603 Kuala Lumpur, Malaysia, and also with the Centre of Advanced Manufacturing & Material Processing (AMMP), 50603 Kuala Lumpur, Malaysia. Contact e-mail: erfan@um.edu.my ABDELMAGID SALEM HAMOUDA, Professor, is with the Mechanical and Industrial Engineering Department, College of Engineering, Qatar University, P.O. Box 2713, Doha, Qatar. GHADER FARAJI, Assistant Professor, is with the School of Mechanical Engineering, College of Engineering, University of Tehran, 11155-4563 Tehran, Iran. MOHSEN ABDELNAEIM HASSAN MOHAMED, Associate Professor, is with the Department of Mechanical Engineering, Faculty of Engineering, University of Malaya and Centre of Advanced Manufacturing & Material Processing (AMMP), and also with the Department of Mechanical Engineering, Faculty of Engineering, Assiut University, Assiut 71516, Egypt.

Manuscript submitted July 9, 2014.
Article published online February 18, 2015

Currently, ECAP is the most common SPD technique. In this process, a workpiece with circular cross section is pressed into a special die. The die consists of the two channels with equal cross section, intersected by an abrupt angle. When workpiece passes through this abrupt angle, intense shear stress is imposed onto the workpiece, while the initial diameter of the workpiece has remained unchanged.[13] Repetitive pressing leads to accumulation of shear strain in the workpiece, and ultimately, a workpiece with UFG structure is produced. In order to enhance the efficiency of the ECAP process in producing refined structures, as well as to adopt this technique to mass production, a number of modified techniques have been developed in recent years.[14]

The UFG metals produced by SPD cannot be produced by conventional thermomechanical treatment (TMT). As a consequence, SPD-processed metals demonstrate suitable combinations of mechanical properties compared with the CG metals manufactured by conventional TMTs.[14] However, conflicting results were reported for the ductility. While some researchers have reported UFG structure show lower ductility compared with CG structure, several observations have reported improvement in the ductility of the UFG structure processed by SPD techniques.[15,16]

Non-age-hardenable aluminum alloys including AA5xxx are not responsive to the SPD process.[17] On the other hand, grain refinement, tensile strength, ductility, and surface hardness enhancement, and also improvement of fatigue life for age-hardenable aluminum alloys such as AA6xxx series are efficiently obtained by the SPD process.[18,19]

For prospective engineering applications of AA6063, the occurrence of potential resistance under small-amplitude oscillatory motion between mating surface subjected to vibration or cyclic loads in combination with fretting fatigue (cyclic bulk fatigue load) needs to be considered along with tensile strength and ductility under monotonic load.[20]

The objective of this research is to evaluate the influences of SPD, HT, and HA on the mechanical properties of AA6063. ECAP (the most successful and common SPD method) was used in this research to produce a UFG structure. Subsequently, the processed parts were heat treated and anodized, and finally, the plain and fretting fatigue lives of the coated and uncoated samples with UFG were investigated.

II. NUMERICAL ANALYSIS OF ECAP

The deformation procedure during the ECAP process was investigated by applying a commercial elastoplastic FEM code (Abaqus/Explicit 6.11; Simulia). Figure 1 illustrates the schematic diagram of ECAP process, where Φ is the die channel angle that usually ranges from 90 to 150 deg, and Ψ is the die corner angle which ranges from 0 deg to 180 deg-Φ.[7] The die channel angle and corner angle considered in this research were 90 and 37 deg, respectively. Selection of these angles is based on evolution of equivalent plastic strain (EPS)[21] and strain

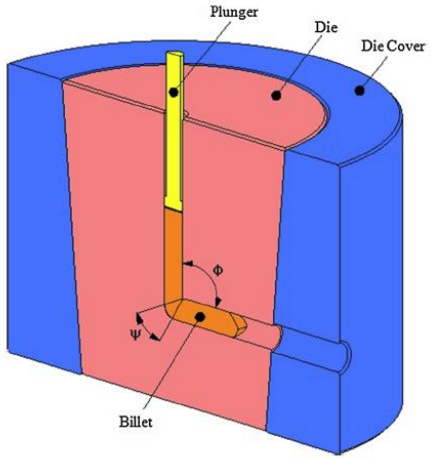

Fig. 1—Pictorial drawing of equal channel angular pressing (ECAP).

inhomogeneity[22] in workpiece after the ECAP process. The values of EPS and the strain inhomogeneity in the current research work are calculated in detail in Section IV–A.

In ECAP process, extreme shear strain is produced in the workpiece during pressing, leading to a UFG structure. To evaluate grain refinement by SPD process, EPS is used as an indicator where a higher EPS indicates finer grains. The strain value, ε, imposed on the sample in ECAP is estimated by an analytic formula incorporating the Ψ (corner angle: representing the outer arc of curvature where the two parts of the channel intersect) and Φ (channel angle: representing the angle between the two parts of the die channel). The relationship is given by Eq. [1] according to[23] as follows:

$$\varepsilon = (P/\sqrt{3})\left[2\cot\left(\frac{\Phi}{2}+\frac{\Psi}{2}\right)+\Psi\,\mathrm{cosec}\left(\frac{\Phi}{2}+\frac{\Psi}{2}\right)\right], \quad [1]$$

where P is the number of pressing passes. For $\Psi = 37$ deg and $\Phi = 90$ deg, Eq. [1] gives the EPS of ~1 in one pass.

FE analysis of ECAP was carried out to identify deformation pattern and distribution of the EPS in the workpiece. The mechanical properties and geometrical dimensions of FE model and experimental procedure were considered to be the same in order to facilitate the comparison between numerical and experimental results. The specimen was meshed into 6200 brick elements with reduced integration (C3D8R) such that, throughout the process, the billet could produce reasonable results under severe deformation. Furthermore, Arbitrary Lagrangian–Eulerian adaptive (ALE) remeshing was utilized throughout the simulation to maintain a high-quality mesh under ECAP by allowing the mesh to move independently with respect to the underlying material.[24] The die set and plunger were modeled as analytic rigid parts.[25,26]

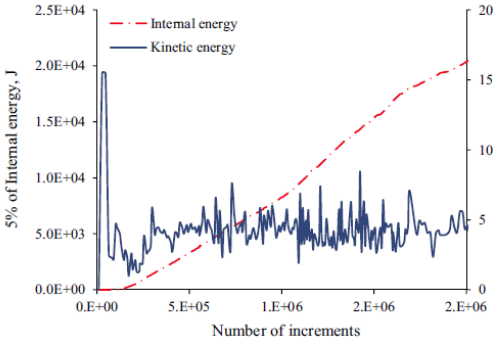

Fig. 2—Variation of kinetic energy *vs* 5 pct of internal energy during ECAP process.

The material used for billet in the simulation was AA 6063-O. The hardening behavior of the materials throughout the FEA was described by $\sigma = 40\varepsilon^{0.15}$ obtained experimentally using tensile test data. Young's modulus, Poisson's ratio, yield stress, and density values are 65 GPa, 0.33, 34.2, and 2700 kg/m^3, respectively. The contact between the tools and the specimen was modeled using the penalty scheme and Coulomb friction with a friction coefficient (μ) of 0.1.

The computational efficiency of the simulation in the explicit procedure was increased by artificially increasing the material density using the mass scaling by factor of 50. In order to avoid errors in the results due to the amplified inertia forces, the ratio of kinetic energy to internal energy was monitored to confirm the quasistatic response of the explicit method.

The kinetic energy of deforming material should not exceed 5 pct of internal energy throughout the simulation, however, in early increments of explicit analysis, an increase of kinetic energy can be neglected due to movement of deformable body before start of significant deformation.[24] The variation of kinetic energy and 5 pct of internal energy during the ECAP process are illustrated in Figure 2. As can be clearly seen from the graph, the value of kinematic energy is significantly below the 5 pct of internal energy except at early increments of simulation, where deformable part is just pushed into the die cavity without having deformation. As an example, in the increment 5.E+05, the value of kinetic energy is almost 5J, while the 5 pct of internal energy is around 4.0E+03.

In order to visualize the convergence of solution in this simulation, the variation of strain energy *vs* the process period for different mesh size was controlled.[27] As an initial run, billet was meshed by 1300 C3D8R elements, and the variation of strain energy was monitored during the simulation. This analysis was terminated during simulation due to excessive mesh distortion as a result of using coarse mesh. The mesh-refinement process was repeated to obtain unchanged value for strain energy. In this regard, five other simulations with total element numbers of 2300, 3200, 4200, 5200, and 6200 were carried out, and the variation

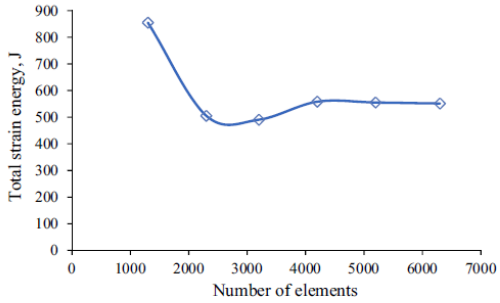

Fig. 3—Variation of total strain energy vs number of elements in model.

Table I. Details of Processes Used in the Current Study with Corresponding Nomenclatures

Sample	Process Nomenclature
1	as-received (raw material)
2	HT
3	SPD
4	SPD + HT
5	SPD + HT + HA

of the strain energy during the simulation was controlled. The variations of total strain energy *vs* element numbers are summarized in Figure 3. As shown in the graph, the analyzed solution converges for models, which were mesh with the total number of elements greater than 4200.

III. EXPERIMENTAL DETAILS

In this study, the influences of heat treatment and hard-anodized coating on mechanical properties, and fatigue and fretting fatigue lives of the ECAPed sample were investigated. In this regard, five sample types were prepared for experimental investigation. Sample types and related nomenclature used in this investigation are summarized in Table I.

A. *ECAP Processing*

The ECAP process was carried out using a die set fabricated with cold-worked steel, heat treated to hardness of 60 HRC and machined with surface roughness of 0.8 μm. Corner angle (Ψ) of 37 deg and channel angle (Φ) of 90 deg were confirmed by FE analysis in advance. The maximum value of EPS and the homogeneity of EPS obtained from FEA were considered as two important parameters for selection of these two angles.

The experiments were conducted using commercial AA6063 having chemical composition and mechanical properties as tabulated in Table II. ECAP billets were cut from the rod with a length of 110 mm and a

Table II. Chemical Composition and Mechanical Properties of the As-received AA 6063-O

Chemical Composition (Wt pct)							Mechanical Properties				
Al	Mg	Si	Fe	Mn	Zn	Cu	σ_y (MPa)	σ_{uts} (MPa)	E (GPa)	υ	ε_{uts}
Balance	0.49	0.45	0.2	0.05	0.02	0.01	34.2	72.7	65	0.33	11.3

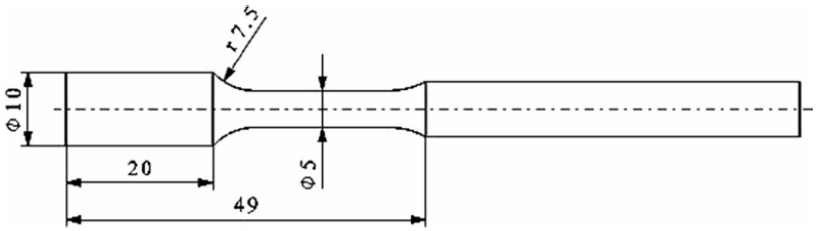

Fig. 4—Geometry of the fretting fatigue specimens according to ISO 1143:2010(E).

diameter of 10 mm along the extrusion direction of the as-received rods for ECAP processing.

Influence of internal heating during ECAP process was investigated by Pei *et al.*[28] Results indicated that for pressing speeds of 0.18, 1.8, and 18 mm s^{-1} temperature rises of about 1 K, 45 K, and 75 K (1 °C, 45 °C, and 75 °C) occur in aluminum alloy billets, respectively. The ECAP process in this research was carried out at room temperature under constant pressing speed of 0.3 mm s^{-1} which considerably minimizes heat generation during deformation. Furthermore, die and billet surfaces were lubricated using MoS_2, to minimize the frictional effects on contact surfaces.

One pass of ECAP was considered for all samples since the maximum increase of ultimate tensile stress occurs in the first cycle and subsequent passes significantly decrease sample ductility.[14]

B. *Heat Treatment*

T4 heat-treatment conditions were considered for the as-received and ECAPed samples. In T4 process, the samples were solution treated at 793 K (520 °C) for 1 hour and instantaneously quenched by water.

C. *Sample Preparation for Fretting Fatigue Testing*

Following the ECAP process, all specimens were machined in accordance with the ISO 1143:2010(E) standard at an initial surface roughness of $R_a = 0.6 \pm 0.1\,\mu m$ by CNC lathe turning machine to study the plain and fretting fatigue lives.[29] All specimens were subsequently polished with 800/2400 grit silicon carbide paper. Dimensions of the fretting fatigue specimens are shown in Figure 4.

D. *Hard-anodizing Procedure*

The HA process is similar to conventional sulfuric anodizing, except that it is done at reduced temperatures, higher unit amperage, and higher final voltage. The oxide layer (Al_2O_3) is the same as that formed in other anodizing processes, with the distinction being that it is much thicker than any other hitherto obtainable.

Initially, samples surface preparation included cleaning to eliminate surface contamination. In the first stage, minor surface imperfections and remaining lubricant particles were removed with hot sodium hydroxide solution. To remove smut (surface oxide), an aqueous solution was used containing simple and complex fluoride ions, an oxidizing inorganic acid, phosphoric and sulfuric acids, manganese in its oxidation state, and an organic carboxylic acid with 1 through 10 carbon atoms. Eventually, concentrated aqueous mixture of nitric and phosphate acids was used to smooth the sample's surface. A near-mirror surface was obtained by this solution. Subsequent to surface cleaning, the workpieces were suspended in electrolytic bath (sulfuric acid diluted by distilled water) as an anode, and direct current was passed through the bath, so that oxygen and hydrogen were produced at the anode surface (workpiece) and at the cathode (graphite), respectively. As a result of this chemical reaction, a layer of alumina (Al_2O_3) was created on the surface of workpieces. The anodizing operating parameters are tabulated in Table III.

The oxygen reacted with the anode (workpiece) to form a durable and abrasion resistant thin aluminum oxide (Al_2O_3) layer, while hydrogen was simultaneously produced at the cathode. The HA process produced a uniform, dense and significantly hard oxide layer (coating) on the workpiece surface compared with a natural oxide layer. A schematic of the HA process is depicted in Figure 5.

E. *Fretting Fatigue Test*

A fretting fatigue specimen was gripped by the chuck and bearing, and loaded rotationally in the in-house

Table III. Hard Anodizing Operating Parameters

Electrolyte	Temperature [K (°C)]	Current Density (A/dm^2)	Voltage (V)	Time (min)
Sulfuric acid (15 wt pct)	273.15 (0)	2	30	30

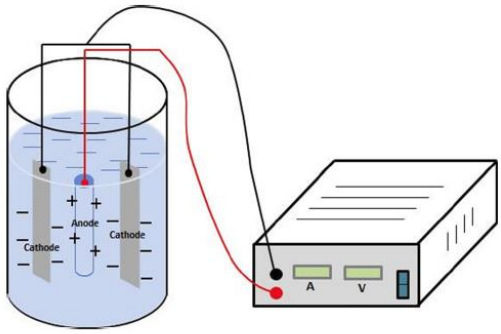

Fig. 5—Schematic diagram of the hard anodizing process.

developed rotating–bending test machine.[30,31] The contact force between the specimen and contact pads was adjusted by application of the fretting ring's screw using torque wrench.

An AISI 4140 steel flat bar with 300 HV hardness, ultimate tensile strength (σ_{uts}) of 700 MPa and yield strength (σ_y) of 420 MPa was used to fabricate the fretting fatigue pads. The specimen material is softer than the pads but the hard-anodized coatings (310 HV) are harder than pads.[32] To simulate the fretting fatigue condition, bridge-type friction pads and a ring-shaped load cell were designed and constructed. The schematic of the fretting fatigue test ring and friction pads is depicted in Figure 6. The fretting fatigue test apparatus was applied at a frequency of 50 Hz and constant contact pressure of 100 MPa at room temperature to attain S/N curves. The nominal maximum cyclic stress was set at a value expected to result in fatigue life between 10^4 and 10^7 cycles. Endurance limit of 1×10^7 cycles was considered for current test according to References 15, 33. The stress required to produce fretting was transmitted to the contact area *via* a calibrated proving ring as schematically illustrated in Figure 6 through the loading pads. Two bases (contacting surfaces) were considered for each loading pads, through which the load was imposed onto the sample. The pad span (distance between the centers of the fretting pad's feet) of 6.8 mm was selected. The pad's base width was 2 mm. The loading pads revolved accompanied by the sample, and this simulates the fretting fatigue conditions between the sample and pads.

Normal force was imposed onto the sample by an adjustable screw and was measured by a load cell. The frictional force created by this normal force had to be calibrated before testing. In order to calibrate the testing load, two strain gages in the direction of friction and another two strain gages at a right angle to this direction were attached to the pads and wired to create a

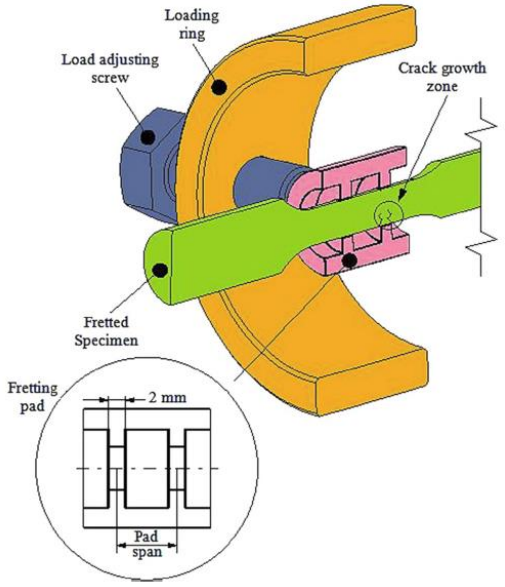

Fig. 6—Assembly of fretted specimen with rotating–bending fretting fatigue machine.

Wheatstone bridge circuit to measure the elastic strain induced by frictional force. This configuration of strain gages cancels out the effects of rising temperature due to the friction at the contact surfaces. Figure 7 shows the force–displacement calibration curve for the current research. This curve was obtained by repetition of several load cases in order to calibrate the frictional force *vs* displacement.

IV. RESULTS AND DISCUSSION

A. *FEA*

Based on the results obtained from FEA, influence of die geometry on billet deformation pattern, amount of EPS imposed on the billet, the pattern of variation in EPS along prescribed paths and EPS inhomogeneity are discussed in this section.

Figure 8 illustrates the plastic deformation zone, steady state zone and corner gap (gap between die internal surface and billet) in the ECAP process. Die channel angle (Φ) and billet material properties are the two most effective parameters that control the work piece deformation pattern and formation of corner gap.[34] According to the results obtained from FEA, a die with channel angle (Φ) of 90 deg produces the

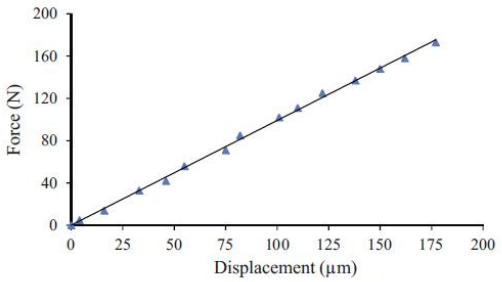

Fig. 7—Force-displacement's calibration curve for the friction pads load cell.

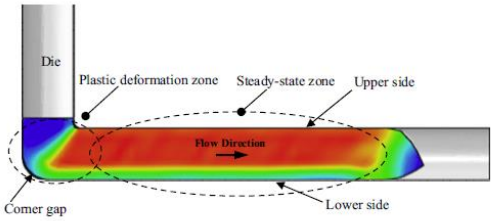

Fig. 8—Major zones of ECAPed billet using die with Ψ = 37 deg and Φ = 90 deg.

minimum corner gap, which is in accordance with the result reported by.[22]

It has been well established that in materials with medium or high stacking fault energies such as aluminum alloys the grain refines effectively as a consequence of continued straining.[35] According to the results obtained from FEA, as a consequence of strain accumulation in billet during ECAP processes an enhancement in mechanical properties of billet can be expected. Figures 9(a) through (d) shows the distribution of EPS in the processed billet for punch strokes 0, 10, 45 and 75 mm, respectively. As is obvious from Figure 9, significant high amount of EPS is accumulated to the billet as it passes through the die abrupt angle. In this regard, the approximate strain introduced to the billet is ~0.98 which is consistent with the result obtained from analytic calculation presented by Eq. [1].

As is obvious from Figure 9, the distribution of EPS is not uniform in the processed billet. To evaluate this nonuniformity in EPS distribution, a virtual plane perpendicular to the flow direction in steady-state zone was considered to quantify the EPS variation. Over this plane, two paths along the outer circumferential direction and the diameter of the pressed billet were defined. These distributions are illustrated in Figure 10.

It is clearly seen in Figure 9 that distributions of EPS at the cross section of the billet after ECAP are nonuniform and have similar trends along the outer circumferential and diametric paths. The EPS value in the upper side (Figure 8) reached a maximum value of ~1.1, while in the lower side, it dropped to the minimum value of ~0.6.

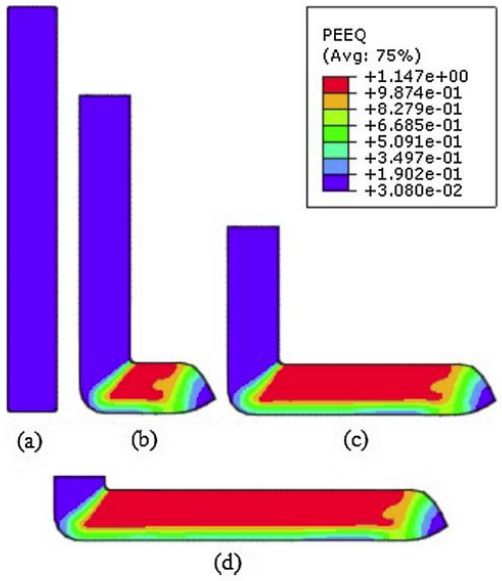

Fig. 9—FE results for equivalent plastic strain distribution in a billet under ECAP: stroke (*a*) 0 mm, (*b*) 10 mm, (*c*) 45 mm, and (*d*) 75 mm.

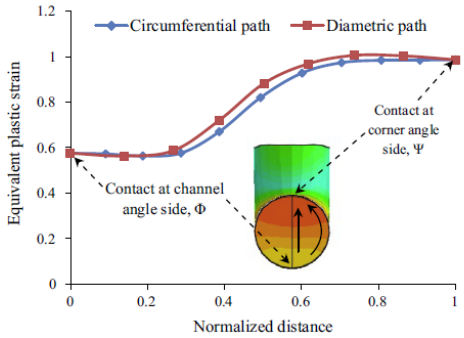

Fig. 10—Distribution of EPS in diametric and circumferential paths at the cross section of a billet after ECAP.

Microstructure homogeneity and hardness uniformity are proportional to homogeneity of the EPS, which is imposed on the billet by SPD process.[36,37] Strain inhomogeneity index (C_i) has been proposed by Li *et al.*[38] as a factor to quantify the degree of deformation inhomogeneity as follows:

$$C_i = \frac{\bar{\varepsilon}^P_{max} - \bar{\varepsilon}^P_{min}}{\bar{\varepsilon}^P_{ave}}, \qquad [2]$$

where $\bar{\varepsilon}^P_{max}$, $\bar{\varepsilon}^P_{min}$, and $\bar{\varepsilon}^P_{ave}$ indicate the maximum, minimum, and average effective plastic strains, respectively. Die channel angle (Φ) and die corner angle (Ψ)

are the origin of the inhomogeneity behavior in ECAP process.[39] The evaluation of C_i for different die configurations indicated that increasing die channel angle (Φ), decrease the C_i values, while having a reverse effect on amount of EPS accumulated in the billet.[34] Inhomogeneity index,C_i in the steady-state zone is almost 0.52 for the current design (Ψ = 37 deg and Φ = 90 deg), which provides acceptable strain homogeneity in billet compared with results obtained for different die configuration by Rajasekaran *et al.*[22]

B. *Mechanical Properties*

In order to investigate the tensile strength and ductility of the samples indicated in Table II, a number of tensile tests recommended by ASTM Standard E8 were performed. The tensile test results are illustrated in Figure 11.

In ECAP process, the grains are refined as a result of extreme EPS which is imposed on the billet. The submicron size grains prohibited the dislocation movement more effectively. Grain size and metal strength are described by the Hall–Petch relationship.[40] As indicated in Figure 11, the yield strength of the sample processed by SPD (sample 3) significantly improved by almost 300 and 95.4 pct in comparison with the as-received material (sample 1) and HT material (sample 2), respectively. However, improvement in the ultimate tensile strength occurred for the samples 4 and 5 as a result of heat treatment after the SPD process.

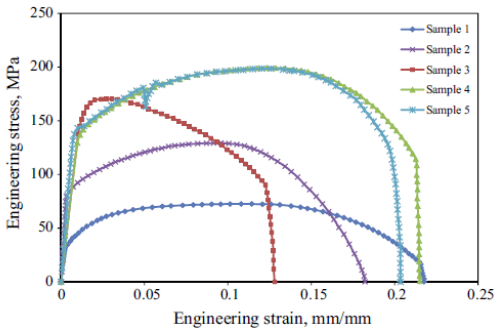

Fig. 11—Engineering stress–strain curves for samples from 1 to 5.

An abrupt drop in stress–strain curve of the sample 5 (HA-coated sample) was observed after a strain of about ε = 0.05. In the case of uncoated samples (samples 1 through 4), as result of continuing extension, strain localization in sample deformation length and a reduction in the cross-sectional area of the sample occur uniformly until necking point. However, in the case of the coated sample (sample 5), as a result of different material properties of coated layer (Al_2O_3) and substrate material (AA6063), series of cracks are nucleated in coated layer (brittle layer). These cracks in coated layer are accumulated, and sudden fracture in coated layer occurs. This phenomenon can be attributed to the observed drop in stress–strain curve of the sample 5.

The data obtained for the presentation of tensile ductility following SPD processing are rather contradictory. While some researchers reported enhanced tensile ductility after SPD owing to the combination of UFG size effects and high-density dislocations in a new mechanism,[16] several others claimed that after the SPD process, low tensile ductility is shown due to strong strain of localization materials.[15] Tensile test results indicate that SPD process improves the yield strength (0.2 pct offset strength), while having a slight detrimental effect on ductility (elongation at break). Tensile test results show that the yield strength of the sample 3 (SPD processed) increased by ~ 90 pct compared with the sample 2 (heat treated); however, heat treatment following the SPD process does not improve the yield strength. Yield strength values for the samples 4 and 5 confirm this finding. Results also show that the SPD process has no significant negative effect on ductility of the AA6063. A significant improvement of ~ 65 pct in ductility of the SPD-processed AA6063 can be obtained by considering the post heat-treatment process.

Concerning fatigue behavior, an increase in the strength of metallic alloys in nanostructured state justifies the exception for fatigue-strength enhancement as well; however, the probability of decreasing tensile ductility must be carefully considered.

A Shimadzu microhardness test machine was used to measure the samples' surface hardness. The average surface hardness value of each sample was achieved from three different points on the sample's surface area. Also, to investigate the variation of surface hardness across the rod surface area after SPD, microhardness testing was carried out on three equidistant points in longitudinal direction. The microhardness results are tabulated in Table IV.

Table IV. Details of Mechanical Properties in the Current Study with Corresponding Nomenclatures

	Tensile Properties				
Samples	Yield Stress (MPa)	Ultimate Stress (MPa)	Strain at Peak Stress (Pct)	Strain at Break Point (Pct)	Micro Hardness (HV)
Sample 1	34.2	72.7	11.3	21	34
Sample 2	70	130	7.3	14	65
Sample 3	136.8	171.1	2.7	13.4	85
Sample 4	135.3	199.8	12.8	22.3	105
Sample 5	138	198	12.5	19.2	310

Link to Full-Text Articles:

http://download-v2.springer.com/static/pdf/962/art%253A10.1007%252Fs11661-015-2806-7.pdf?token2=exp=1429585314~acl=%2Fstatic%2Fpdf%2F962%2Fart%25253A10.1007%25252Fs11661-015-2806-7.pdf*~hmac=2c4afb03442593f65738e81a109f1427d5220c08144281708f42d250e4a41a88